

## Machine Learning Assisted Mechanical Metamaterial Design for Additive Manufacturing

Jier Wang\*, Ajit Panesar\*

\*IDEA Lab, Department of Aeronautics, Imperial College London, UK

### Abstract

Metamaterials, widely studied for its counterintuitive property such as negative Poisson's ratio, negative refraction, negative thermal expansion, and employed in various fields, are recognised to provide foundation for superior multiscale structural designs. However, current mechanical metamaterial design methods usually rely on performing sizing optimisations on predefined topology or implementing time-consuming inverse homogenisation methods. Machine Learning (ML), as a powerful self-learning tool, is considered to have the potential of discovering metamaterial topology and extending its property bounds. This work considers the use of Neural Networks (NNs), (De-Convolutional Neural Networks) DCNNs and Generative Adversarial Networks (GANs) to speed up the generation of new topologies for metamaterials. NNs and DCNNs are trained to inversely generate metamaterial designs based on the input target effective macroscale properties, whilst the generator in GANs is expected to output diverse metamaterial microstructures with random noise inputs. This work highlights the potential of data-driven approaches in Design for Additive Manufacturing (DfAM) as an alternative to the time-consuming, conventional methods.

### Introduction

Metamaterials are structures that are designed to exhibit extraordinary mechanical, electromagnetic, optical, or other properties not found in natural materials. Auxetic materials are a category of mechanical metamaterials which have negative Poisson's ratios [1] (i.e. materials would expand under tension, while compact under compression [2]). Auxetic metamaterials can be potentially applied in various fields, like aerospace, biomedical, sport wears, automobile, vehicles, etc. Additive Manufacturing (AM) provides larger manufacturing flexibility and facilitates the complex design of structures [3]–[6]. Metamaterials, which usually rely on complex microscale architectures to achieve unusual properties at the macro-scale, would benefit from AM.

A few classes of auxetic metamaterials have been reviewed in [1][7], including re-entrant models [8]–[10], rotating polygonal models [11][12], chiral models [13], crumpled sheets models [14], perforated sheets models, etc. Apart from existed templates, an automated way using a numerical topology optimisation method to design periodic microstructures possessing prescribed elastic properties was proposed in [15]. The design objective of this topology optimisation method is to minimise the error between obtained elastic properties and prescribed properties with a constraint on material volume.

Machine Learning (ML) as a fast-developing technique, has attracted immense attention in the past few years. Several different roles of ML in structural design have been discussed in [16]. ML, in contrast to physics-based methods, has demonstrated its superior efficacy in exploring and extending microstructure design domain. For instance, ML showed its capability of automatically discovering microstructures which exhibit extremal elastic macroscale properties in [17]. Similarly, a self-learning algorithm for a given hierarchical material to hone on superior microstructure designs which can achieve higher strength and toughness was proposed [18]. K-means clustering was adopted to cluster the elements to 3 or 4 cell clusters based on elemental densities before the subsequent micro-structure optimisation of each cluster [19]. Autoencoder was employed to predict mechanical properties of a micro-lattice using the encoder and to generate micro-lattices from the desired mechanical properties using the decoder [20]. Neural Networks (NNs) were deployed to establish relations between regular triangular lattice structure and its elasticity properties for the design of architected lattices with tunable anisotropy [21]. Convolutional Neural Networks (CNNs) are applied to de-homogenisation method to reduce computational cost and seek for possibility in future interactive high-resolution topology optimisation [22].

ML was found to provide DfAM with extraordinary structural designs in our early work [23], where the well-trained NNs-based inverse generator has been proved to have the capability of generating 2D lattice cells with desired mechanical property and achieving high-efficient graded lattice design when combined with TO. Moreover, ML-based inverse design has greater potential to be explored, as advanced ML methods could provide extra functionalities to structural design cases.

In this work, a type of auxetic metamaterial from re-entrant model class is adopted as an example to provide insights in the utilisations of ML in metamaterial inverse design. The aim is to inversely generate microstructural designs that perform desired properties, which are prescribed elastic constitutive matrix with negative Poisson’s ratios. Different types of ML models are adopted and compared to show the advantages and potentials in metamaterial design, including NNs, De-Convolutional Neural Networks (DCNNs), and Generative Adversarial Networks (GANs).

The paper follows the following structure. Firstly, the adopted auxetic metamaterial structure is introduced, accompanied by an overview of the data collection process and the dataset sizes. Subsequently, the main methodologies employed for the inverse generation of auxetic metamaterials using three proposed machine learning (ML) models are presented, including detailed explanations of the model training and testing procedures. Finally, a comparison of results from different ML models is conducted, taking into account accuracy metrics as well as computational costs.

## Methodology

### **Auxetic Metamaterial Candidate**

This work focuses on an example of 2D auxetic metamaterials, which are pixelised with a resolution of  $28 \times 28$  (see Figure 1 for a repetitive base unit cell).

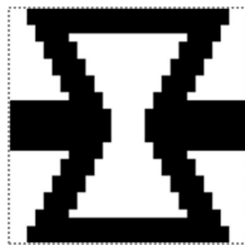


Figure 1: An example of auxetic metamaterial adopted

The shape of the microstructure is controlled by three parameters  $h$ ,  $d$ ,  $t$  (see Figure 2).

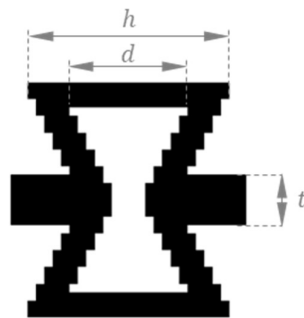


Figure 2: Illustration of nodal parameters for re-entrant honeycomb cell

In this study, the focus is on the effective macroscale elastic property of the microstructure, which is characterized by the constitutive matrix  $\mathbf{D}$ :

$$\boldsymbol{\sigma} = \mathbf{D}\boldsymbol{\varepsilon} \quad (1)$$

where  $\boldsymbol{\varepsilon}$  is the strain,  $\boldsymbol{\sigma}$  is the stress.

For 2D anisotropic material, because of the symmetry of the  $\mathbf{D}$  matrix, there are 6 independent variables in  $\mathbf{D}$ . These 6 independent variables are represented using  $D_{11}, D_{12}, D_{13}, D_{22}, D_{23}, D_{33}$  in this paper, where  $D_{ij}$  refers to component in the  $i$ -th row and  $j$ -th column. Considering the re-entrant honeycomb auxetic metamaterial cell type adopted, it can be derived that:

$$D_{13} = 0, D_{23} = 0 \quad (2)$$

Therefore, four parameters ( $D_{11}, D_{12}, D_{22}, D_{33}$ ) are used to represent the constitutive matrix  $\mathbf{D}$ . In the case of auxetic metamaterials, it is expected that the value of  $D_{12}$  is negative. The homogenisation method [24] is employed to compute the effective elastic properties of the auxetic metamaterial designs.

To create the dataset for ML training and testing, the three parameters  $h, d, t$  are randomly generated with upper and lower bounds:

$$\begin{aligned} S \quad & d + 0.25a < h < 0.9a \\ & 0.1a < d < 0.6a \\ & 0.05a < t < 0.3a \end{aligned} \quad (3)$$

where  $a$  is the length of unit cell.

A dataset of size 5000 was collected, which was then randomly divided into a training dataset consisting of 4000 samples and a testing dataset containing 1000 samples. In order to augment the dataset further, diagonal flipping of the unit cells, as shown in Figure 3, resulted in an additional 5000 data points. These flipped unit cells can be incorporated into the training dataset as another metamaterial type when training pixel-based machine learning methods such as DCNNs and GANs.

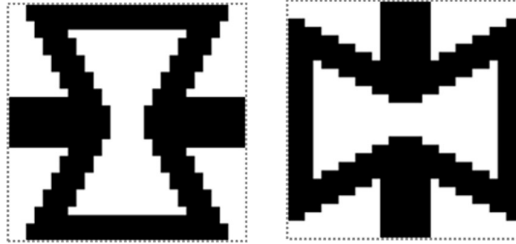


Figure 3: Original cell and flipped cell

### Structures of ML Models

Three different types of ML models are considered herein, which are NNs, DCNNs, and GANs. NNs deal with 1-dimensional inputs and outputs, which requires the predefinition of cell type, whilst DCNNs and GANs can output pixel-based images. Different model structures are explained in detail:

### Fully-connected NNs

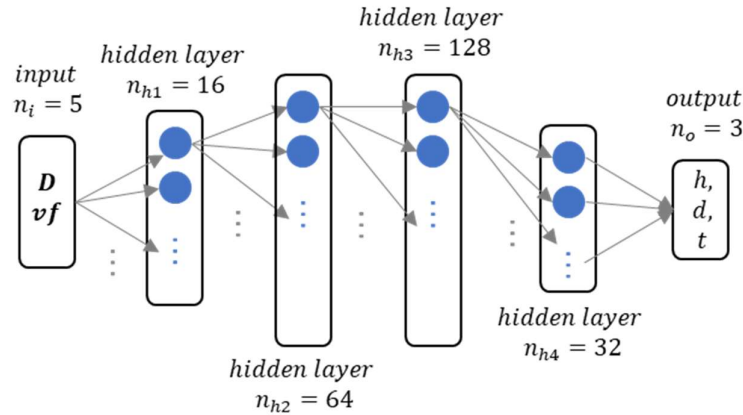


Figure 4: Illustration of NNs structure

A structure of the NN for this auxetic metamaterial inverse generator problem is shown as Figure 4. The inputs are constitutive matrix ( $D_{11}, D_{12}, D_{22}, D_{33}$ ) and the volume fraction ( $vf$ ) of microstructure, while the output is the 3-dimensional cell parameter controlling the unit cell shape. The hidden layer number and number of neurons in each layer are pre-determined as a trade-off between training time and model accuracy. Adjustment would take place if the evaluation of the trained model is not satisfactory. The finally adopted NN structure has four hidden layers, with 16, 64, 128, 32 neurons respectively and 13731 total training parameters. By leveraging the benefits of 1-dimensional data structures, it is possible to deliberately restrict the total number of training parameters to a smaller magnitude, which plays a crucial role in effectively managing the computational cost at a lower level.

### DCNNs

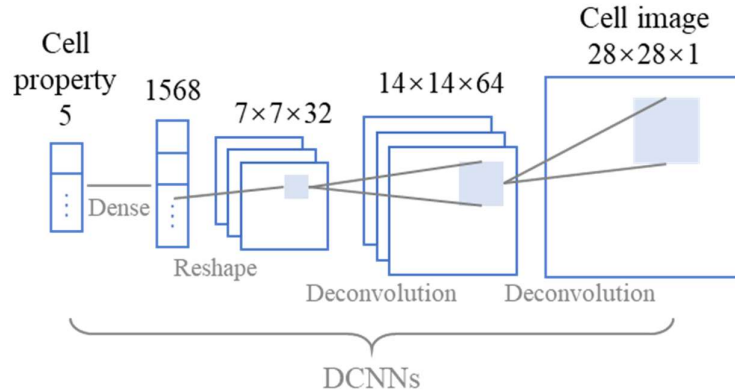


Figure 5: Illustration of DCNNs structure

As shown in Figure 5, de-convolution layers (also called as transposed convolution layers) are used in the DCNNs model to construct the metamaterial inverse generator. During the training process, the loss function is formulated to quantify the disparity between the reconstructed cell topology and the original cell topology. By representing the metamaterial unit cell designs as pixel-based images, DCNNs possess the capability to handle diverse cell types with one single model. In this particular DCNNs architecture, the dimensions of output images remain constant, while additional layers can be incorporated to facilitate the conversion of the image to user-defined resolutions. An increase in the desired output image size necessitates a more intricate DCNNs structure, resulting in higher computational requirements.

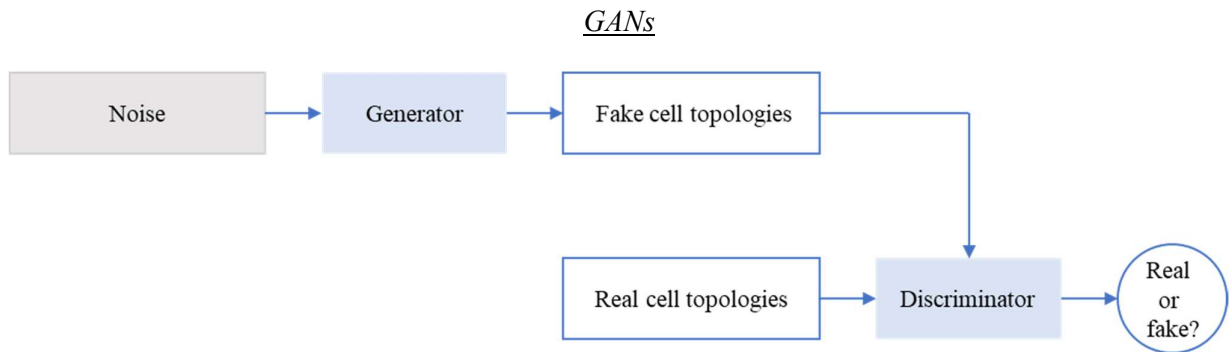


Figure 6: Illustration of GANs structure

Generative adversarial networks (GANs) consist of two components, namely the “Generator” and the “Discriminator”, which act as adversaries. The Generator, serving as an inverse generator for metamaterial designs, is trained to generate realistic images from noise vectors, while the Discriminator is trained to distinguish between the output of the Generator and real data. The Generator is a simple unit cell output model mimicking the random generation of microstructure topology without restrictions. With a series of random noises, the generator is expected to provide several choices. Presently, the structure of GANs does not enforce any specific constraints on cell properties. However, in future research endeavours, conditional GANs (cGANs) will be explored as a means to incorporate cell property requirements as conditions. This integration of conditions will enable the cGANs to function effectively as inverse generators for metamaterial designs.

## Results and Discussions

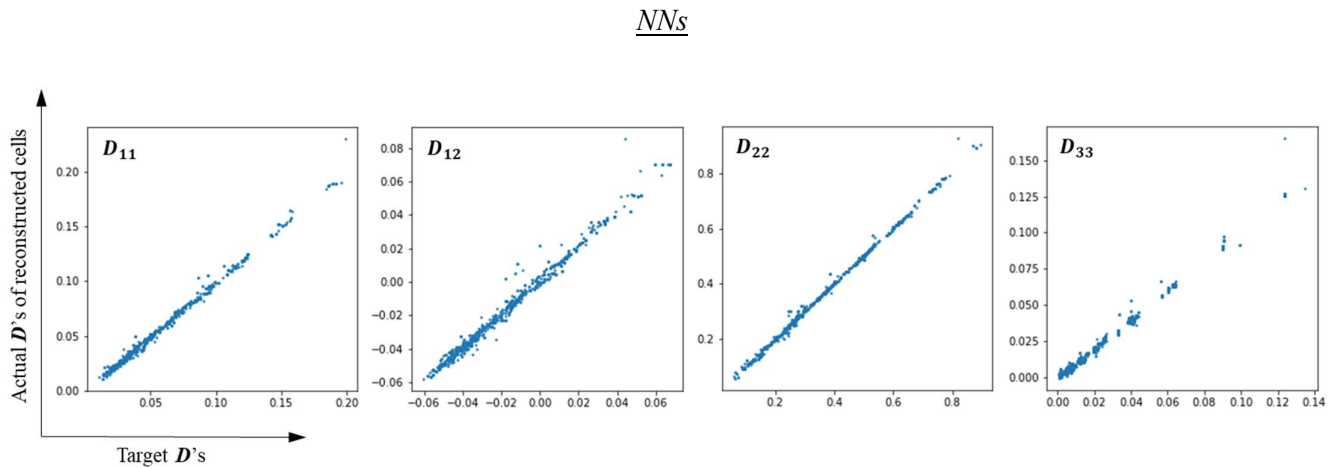


Figure 7: Results from NNs-based inverse generator

The accuracy of the NNs-based inverse generator is assessed by comparing the target  $\mathbf{D}$  (input for the inverse generator) with the actual  $\mathbf{D}$  of the generated metamaterial cells. This comparison is illustrated in Figure 7, where the x-axis represents the target  $\mathbf{D}$  values, and the y-axis represents the corresponding actual  $\mathbf{D}$  values of the output cells obtained from the inverse generator. The  $R^2$  values for all four components of  $\mathbf{D}$  exceed 0.99, indicating a high level of accuracy achieved by the NNs-based inverse generator.

## DCNNs

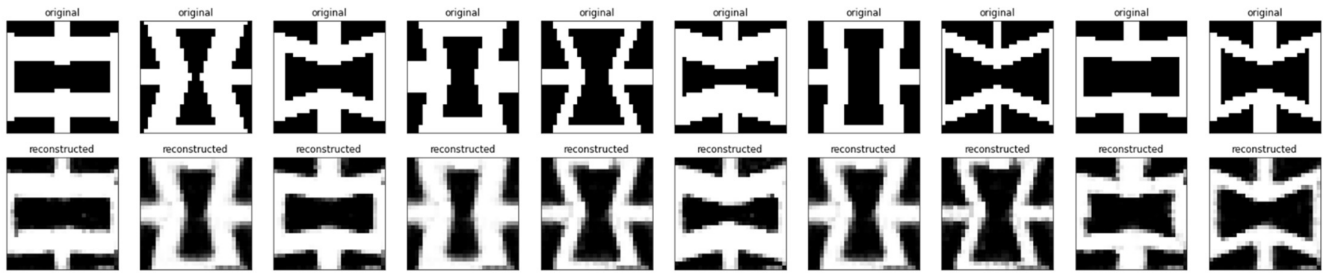


Figure 8: Results from DCNNs-based inverse generator

The DCNNs-based inverse generator is evaluated for model accuracy by comparing the reconstructed metamaterial cells (generated based on the target properties) with the original cells. Figure 8 provides a visual representation of these comparisons, where the first row presents the original cells considered as the ground truth, and the second row shows the output structures generated by the DCNNs-based inverse generator. The figure serves as evidence that the inverse generator effectively handles both the original hourglass type and the diagonal-flipped type of metamaterials, as observed through the comparison.

Pixel-based ML models offer the capability to capture intricate details from discretized structures without predefined cell topologies, which enables the build of general generators. In most cases, when incorporating additional cell types, a larger training dataset is typically needed. In the context of this DCNNs model, it is hypothesised that the amount of additional data required diminishes as the number of species increases. This implies the potential to train a more generalised generator that can effectively handle diverse metamaterial types with a reduced reliance on extensive additional training data.

## GANs



Figure 9: Results from GANs-based generator

Figure 9 depicts the output metamaterial cells generated by the GANs-based generator. It can be observed from the figure that the trained generator is capable of producing metamaterial cells that closely resemble the real cells from the training dataset. This initial experimentation with applying GANs to metamaterial generation provides valuable insights into utilising the generator from GANs as a generator for further exploration of the metamaterial design domain.

To incorporate property requirements, additional conditions can be introduced in conditional GANs (cGANs) to ensure that the generated cells meet the desired specifications. This approach enables the exploration of new, previously unseen metamaterial designs using a more generalised generator. Moreover, the introduction of noise input allows for the generation of diverse cell options, thus facilitating exploration within the design space.

## Conclusion

Metamaterials possess exceptional properties and have garnered significant attention for their potential applications in various fields. The fabrication of metamaterials has improved substantially with the rapid

development of AM, allowing for more complex and precise designs. However, the design strategies for metamaterials need to evolve in order to achieve desired material responses and structural behaviours while minimizing computational time.

This work serves as an extension of previous research on lattice design using an inverse generator, with the objective of exploring the feasibility of applying other advanced ML models to microstructural design problems. Specifically, this study adopts NNs, DCNNs and GANs to assist in the generation of metamaterial cells. Each of these models exhibits distinct advantages as metamaterial generators. NNs offer fast training and high accuracy, particularly suitable for inverse generation with predefined metamaterial types. DCNNs provide pixel-based inverse generation, allowing for the potential development of a generalised generator capable of handling unseen metamaterial types. GANs enables the generation of metamaterial cells from randomly generated noises, opening up possibilities for exploring new metamaterial types. Additionally, the computational cost for training the models increases following the order of NNs < DCNNs < GANs.

In future work, further development of the metamaterial generator will focus on several aspects. Firstly, efforts can be directed towards building a general generator capable of accommodating various metamaterial types. Secondly, exploring unseen metamaterial designs can help uncover novel and innovative designs. Lastly, enhancing compatibility with user-defined resolutions for microscale structures would enable greater flexibility and customisation.

### Reference

- [1] X. Ren, R. Das, P. Tran, T. D. Ngo, and Y. M. Xie, "Auxetic metamaterials and structures: a review," *Smart Mater. Struct.*, vol. 27, no. 2, p. 023001, Jan. 2018, doi: 10.1088/1361-665X/AAA61C.
- [2] X. Cheng *et al.*, "Design and mechanical characteristics of auxetic metamaterial with tunable stiffness," *Int. J. Mech. Sci.*, vol. 223, no. March, p. 107286, 2022, doi: 10.1016/j.ijmecsci.2022.107286.
- [3] J. Plocher and A. Panesar, "Review on design and structural optimisation in additive manufacturing: Towards next-generation lightweight structures," *Materials and Design*, vol. 183, 2019, doi: 10.1016/j.matdes.2019.108164.
- [4] D. Brackett, I. Ashcroft, and R. Hague, "Topology optimization for additive manufacturing," in *22nd Annual International Solid Freeform Fabrication Symposium - An Additive Manufacturing Conference, SFF 2011*, 2011.
- [5] J. ZHU, H. ZHOU, C. WANG, L. ZHOU, S. YUAN, and W. ZHANG, "A review of topology optimization for additive manufacturing: Status and challenges," *Chinese Journal of Aeronautics*, vol. 34, no. 1, 2021, doi: 10.1016/j.cja.2020.09.020.
- [6] W. Gao *et al.*, "The status, challenges, and future of additive manufacturing in engineering," *CAD Comput. Aided Des.*, vol. 69, 2015, doi: 10.1016/j.cad.2015.04.001.
- [7] W. Jiang *et al.*, "Manufacturing, characteristics and applications of auxetic foams: A state-of-the-art review," *Compos. Part B Eng.*, vol. 235, no. September 2021, p. 109733, 2022, doi: 10.1016/j.compositesb.2022.109733.
- [8] T. Maconachie *et al.*, "SLM lattice structures: Properties, performance, applications and challenges," *Mater. Des.*, vol. 183, p. 108137, 2019, doi: 10.1016/j.matdes.2019.108137.
- [9] L. Yang, O. Harrysson, H. West, and D. Cormier, "Mechanical properties of 3D re-entrant honeycomb auxetic structures realized via additive manufacturing," *Int. J. Solids Struct.*, vol. 69–70, pp. 475–490, 2015, doi: 10.1016/j.ijsolstr.2015.05.005.
- [10] I. G. Masters and K. E. Evans, "Models for the elastic deformation of honeycombs," *Compos. Struct.*, vol. 35, no. 4, pp. 403–422, 1996, doi: 10.1016/S0263-8223(96)00054-2.
- [11] J. N. Grima and K. E. Evans, "Auxetic behavior from rotating squares," *J. Mater. Sci. Lett.*, vol. 19, no. 17, pp. 1563–1565, 2000, doi: 10.1023/A:1006781224002.
- [12] J. N. Grima and K. E. Evans, "Auxetic behavior from rotating triangles," *J. Mater. Sci.*, vol. 41, no. 10, pp. 3193–3196, 2006, doi: 10.1007/s10853-006-6339-8.

- [13] D. Prall and R. S. Lakes, “Properties of chiral honeycombe with Poisson’s ratio of -1,” *Int. J. Mech. Sci.*, vol. 39, no. 3, pp. 305–314, 1997.
- [14] K. Alderson, A. Alderson, N. Ravirala, V. Simkins, and P. Davies, “Manufacture and characterisation of thin flat and curved auxetic foam sheets,” *Phys. Status Solidi Basic Res.*, vol. 249, no. 7, pp. 1315–1321, 2012, doi: 10.1002/pssb.201084215.
- [15] U. D. Larsen, O. Sigmund, and S. Bouwstra, “Design and fabrication of compliant micromechanisms and structures with negative Poisson’s ratio,” *J. Microelectromechanical Syst.*, vol. 6, no. 2, pp. 99–106, 1997, doi: 10.1109/84.585787.
- [16] R. V. Woldseth, N. Aage, J. A. Bærentzen, and O. Sigmund, *On the use of artificial neural networks in topology optimisation*, vol. 65, no. 10. Springer Berlin Heidelberg, 2022.
- [17] D. Chen, M. Skouras, B. Zhu, and W. Matusik, “Computational discovery of extremal microstructure families,” *Sci. Adv.*, vol. 4, no. 1, pp. 1–8, 2018, doi: 10.1126/sciadv.aao7005.
- [18] G. X. Gu, C. T. Chen, D. J. Richmond, and M. J. Buehler, “Bioinspired hierarchical composite design using machine learning: simulation, additive manufacturing, and experiment,” *Mater. Horizons*, vol. 5, no. 5, pp. 939–945, Aug. 2018, doi: 10.1039/C8MH00653A.
- [19] K. Liu, A. Tovar, E. Nutwell, and D. Detwiler, “Towards nonlinear multimaterial topology optimization using unsupervised machine learning and metamodel-based optimization,” in *Proceedings of the ASME Design Engineering Technical Conference*, 2015, vol. 2B-2015, doi: 10.1115/DETC201546534.
- [20] N. Després, E. Cyr, P. Setoodeh, and M. Mohammadi, “Deep Learning and Design for Additive Manufacturing: A Framework for Microlattice Architecture,” *JOM*, vol. 72, no. 6, 2020, doi: 10.1007/s11837-020-04131-6.
- [21] R. Kulagin, Y. Beygelzimer, Y. Estrin, A. Schumilin, and P. Gumbsch, “Architected Lattice Materials with Tunable Anisotropy: Design and Analysis of the Material Property Space with the Aid of Machine Learning,” *Adv. Eng. Mater.*, vol. 22, no. 12, 2020, doi: 10.1002/adem.202001069.
- [22] M. O. Elingaard, N. Aage, J. A. Bærentzen, and O. Sigmund, “De-homogenization using convolutional neural networks,” *Comput. Methods Appl. Mech. Eng.*, vol. 388, pp. 1–28, 2022, doi: 10.1016/j.cma.2021.114197.
- [23] J. Wang and A. Panesar, “Machine learning based lattice generation method derived from topology optimisation,” *Addit. Manuf.*, vol. 60, no. PB, p. 103238, 2022, doi: 10.1016/j.addma.2022.103238.
- [24] E. Andreassen and C. S. Andreasen, “How to determine composite material properties using numerical homogenization,” *Comput. Mater. Sci.*, vol. 83, pp. 488–495, Feb. 2014, doi: 10.1016/J.COMMATSCI.2013.09.006.